Inorg. Chem. **2005**, *44*, 9068–9075

Inorganic Chemistry
Article

Reactivity of Bis(μ-hydroxo) Divanadium Site in γ-$H_2SiV_2W_{10}O_{40}{}^{4-}$ with Hydroxo Compounds

Yoshinao Nakagawa,[†] Kazuhiro Uehara,[‡] and Noritaka Mizuno*,[†,‡]

Department of Applied Chemistry, School of Engineering, The University of Tokyo, 7-3-1 Hongo, Bunkyo-ku, Tokyo 113-8656, Japan, and Core Research for Evolutional Science and Technology, Japan Science and Technology Agency, 4-1-8 Honcho, Kawaguchi, Saitama, 332-0012, Japan

Received July 12, 2005

The reactivity of divanadium-substituted silicotungstate, γ-$H_2SiV_2W_{10}O_{40}{}^{4-}$ (**I**), with hydroxo compounds of alcohols, carboxylic acids, and water is reported. The reaction of the bis(μ-hydroxo) divanadium site in **I** with primary alcohols and formic acid smoothly proceeds to form corresponding monoesters and monoformate, respectively, and the crystal structures of the monomethyl and monoethyl esters and the monoformate of **I** are determined. The oxygen exchange between the hydroxo group and water proceeds easily. On the other hand, bulky compounds of 2-propanol, *tert*-butyl alcohol, and acetic acid hardly react with the bis(μ-hydroxo) divanadium site (equilibrium constant < 0.01) because of the steric crowding between the methyl groups and the polyoxometalate framework.

Introduction

The coordination chemistry of vanadium(V) has attracted much attention because of the catalytic[1] and bioinorganic[2] importance of vandium compounds. Vanadate esters (vanadium alkoxides) are important complexes as oxidants or oxidation catalysts, oxide precursors, and analogues of phosphate esters in the fields of organic[1,3] and inorganic syntheses,[4] and bioinorganic chemistry,[2,5] respectively. They are also reported to be a key intermediate for the aerobic oxidation of alcohols with vanadia catalysts.[6] Therefore, investigation on reactivity of the vanadium site with hydroxo compounds of alcohols, acid, and water is interesting.

The aqueous chemistry of metal oxoanions, especially vanadates, is complex, and the complexity, in part, comes from the ability of the vanadate ion to undergo protonation and oligomerization.[7−9] The incorporation of vanadium centers to the more stable, rigid polyoxometalate framework may avoid the complex equilibrium. Keggin- ($XW_{12}O_{40}{}^{n-}$) and Dawson-type ($X_2W_{18}O_{62}{}^{m-}$) polyoxotungstates show stability toward hydrolysis or isomerization when dissolved in organic solvents such as acetonitrile.[10] We have recently reported the crystal structure of divanadium-substituted silicotungstate, γ-$H_2SiV_2W_{10}O_{40}{}^{4-}$ (**I**), and the sterically controlled esterification with alcohols.[11] The bis(μ-hydroxo) divanadium site of **I** quickly reacts with primary alcohols under mild conditions to form only monoester, and no diester is formed. In this paper, we report the full details for the reactivity of the vanadium site in **I** with hydroxo compounds including not only alcohols but also carboxylic acids and water. The crystal structures of the monomethyl and -ethyl esters and monoformate forms of **I** are determined.

Experimental Section

General. Dry acetonitrile (water, $<0.005\%$) was purchased from Wako Pure Chemical Industries, Ltd. and was used as received.

---

* To whom correspondence should be addressed. E-mail: tmizuno@mail.ecc.u-tokyo.ac.jp.

[†] The University of Tokyo.

[‡] Japan Science and Technology Agency.

(1) (a) Ligtenbarg, A. G. J.; Hage, R.; Feringa, B. L. *Coord. Chem. Rev.* **2003**, *237*, 89. (b) Conte, V.; Di Furia, F.; Licini, G. *Appl. Catal. A* **1997**, *157*, 335. (c) Butler, A.; Clague, M. J.; Meister, G. E. *Chem. Rev.* **1994**, *94*, 625.

(2) (a) Thompson, K. H.; Orvig, C. *Coord. Chem. Rev.* **2001**, *219−221*, 1033. (b) *Vanadium and Its Role in Life*; Sigel, H., Sigel, A., Eds.; Marcel Dekker Inc.: New York, 1995. (c) Rehder, D. *Angew. Chem., Int. Ed. Engl.* **1991**, *30*, 148.

(3) Hirao, T. *Chem. Rev.* **1997**, *97*, 2707.

(4) (a) Thematic issue on recent advances in metal alkoxide and amide chemistry. *Polyhedron* **1998**, *17*, 623. (b) Bradley, D. C. *Chem. Rev.* **1989**, *89*, 1317.

(5) Crans, D. C.; Smee, J. J.; Gaidamauskas, E.; Yang, L. *Chem. Rev.* **2004**, *104*, 849.

(6) Forzatti, P.; Tronconi, E.; Elmi, A. S.; Busca, G. *Appl. Catal. A* **1997**, *157*, 387.

(7) Gresser, M. J.; Tracey, A. S. *J. Am. Chem. Soc.* **1986**, *108*, 1935.

(8) Jiang, F.; Anderson, O. P.; Miller, S. M.; Chen, J.; Mahroof-Tahir, M.; Crans, D. C. *Inorg. Chem.* **1998**, *37*, 5439.

(9) Crans, D. C.; Schelble, S. M.; Theisen, L. A. *J. Org. Chem.* **1991**, *56*, 1266.

(10) Pope, M. T. *Heteropoly and Isopoly Oxometalates*; Springer-Verlag: New York, 1983.

(11) Nakagawa, Y.; Uehara, K.; Mizuno, N. *Inorg. Chem.* **2005**, *44*, 14.

10.1021/ic051163x CCC: $30.25

The other reagents were of reagent grade and were used as received. IR spectra (KBr pellets) were measured with Perkin-Elmer PARAGON 1000PC spectrometer at room temperature, and UV−vis spectra were measured with Perkin-Elmer LAMBDA 12 spectrometer at room temperature. The NMR spectra of ^{1}H (270 MHz), ^{29}Si (53.5 MHz), ^{51}V (71.0 MHz), and ^{183}W (11.2 MHz) were recorded with a JEOL JNM-270EX spectrometer at 298 ± 0.2 K. Chemical shifts of ^{29}Si, ^{51}V, and ^{183}W were referenced to neat TMS (0 ppm), neat $VOCl_3$ (0 ppm), and Na_2WO_4/D_2O (0 ppm), respectively. Cold-spray mass spectra[12] were measured with JEOL JMS-T100CS spectrometer in the negative-ion mode by direct infusion with a syringe pump (0.05 mL min^{-1}).

Synthesis of $[(n\text{-}C_4H_9)_4N]_4[\gamma\text{-}H_2SiV_2W_{10}O_{40}]\cdot H_2O$ (TBA−I). An aqueous solution of $[\gamma\text{-}SiV_2W_{10}O_{40}]^{6-}$ was prepared according to ref 13, and the anion was isolated as the tetrabutylammonium salt. $K_8[\gamma\text{-}SiW_{10}O_{36}]\cdot 12H_2O$[14] (8 g, 2.7 mmol) was quickly dissolved in 1 M HCl (28 mL). $NaVO_3$ (0.5 M, 11 mL, 5.5 mmol) was added, and the mixture was gently stirred for 5 min and then filtered. $[(n\text{-}C_4H_9)_4N]Br$ (8 g, 25 mmol) was added to the filtrate in a single step, and the mixture was filtered. The resulting yellow precipitate collected was washed with an excess amount of water (300 mL). The crude compound was purified twice by precipitation (i.e., addition of 1 L of H_2O into acetonitrile solution of TBA−**I** (50 mL)). Analytically pure TBA−**I** was obtained as a pale yellow powder. Yield: 7.43 g (76%). Anal. Calcd for $[(C_4H_9)_4N]_4H_2SiV_2W_{10}O_{40}\cdot H_2O$: C, 21.4; H, 4.15; N, 1.56; Si, 0.78; V, 2.83; W, 51.1; H_2O, 0.50. Found: C, 21.4; H, 3.91; N, 1.59; Si, 0.79; V, 2.88; W, 51.2; H_2O, 0.50. ^{51}V NMR (CH_3CN): δ −564 ($\Delta\nu_{1/2}$ = 130 Hz). ^{183}W NMR (CD_3CN): δ −82.2 ($\Delta\nu_{1/2}$ = 9.6 Hz), −95.6 ($\Delta\nu_{1/2}$ = 2.5 Hz), −129.7 ($\Delta\nu_{1/2}$ = 2.9 Hz) with an integrated intensity ratio of 1.9/1.0/2.1. ^{29}Si NMR (CD_3CN): δ −84.0 ($\Delta\nu_{1/2}$ = 2.0 Hz). ^{1}H NMR (CD_3CN): δ 5.07 (2H, s, V−O*H*-V), 3.13 (cation), 1.63 (cation), 1.43 (cation), 0.99 (cation). The UV−vis spectrum (in CH_3CN) showed shoulder bands at 240 (ϵ = 36000 M^{-1} cm^{-1}), 285 (24000), and 350 nm (5900), characteristic of the γ-Keggin structure.[15] IR spectrum (KBr, cm^{-1}): 1151, 1106, 1057, 1004, 995, 966, 915, 904, 875, 840, 790, 691, 550, 519, 482, 457, 405.

Synthesis of $[K(18\text{-}crown\text{-}6)]_4[\gamma\text{-}H_2SiV_2W_{10}O_{40}]$ (CEK−I). $K_8[\gamma\text{-}SiW_{10}O_{36}]\cdot 12H_2O$[14] (1.5 g, 0.5 mmol) was quickly dissolved in 1 M HCl (15 mL). KVO_3 (0.152 g, 1.1 mmol) dissolved in water (10 mL) was quickly added, and the mixture was gently stirred for 5 min and them filtered. 18-crown-6 (0.792 g, 3 mmol) was added to the filtrate in a single step, and the mixture was filtered. The resulting yellow precipitate was washed with a small amount of water. The crude product was purified with the precipitation method (i.e., addition of diethyl ether (40 mL) into acetonitrile solution (50 mL)). Yield: 1.01 g (54%). Crystals suitable for the X-ray analysis were obtained by recrystallization from DMSO/H_2O. Anal. Calcd for $[K(C_{12}H_{24}O_6)]_4[H_2SiV_2W_{10}O_{40}]$: C, 15.1; H, 2.58. Found: C, 15.1; H, 2.52. IR (KBr, cm^{-1}): 1108, 1004, 991, 967, 905, 874, 792, 699, 543, 410. ^{51}V NMR (CH_3CN): δ −563 ppm ($\Delta\nu_{1/2}$ = 130 Hz). ^{1}H NMR (CD_3CN): δ, 5.10 (2H, s, V−O*H*-V), 3.60 ppm (cation).

Synthesis of $[K(18\text{-}crown\text{-}6)]_4[\gamma\text{-}HSiV_2W_{10}O_{39}(\mu\text{-}OCH_3)]$ (CEK−II). CEK-**I** (150 mg, 40 μmol) was dissolved in acetonitrile (10 mL). Methanol (0.4 mL, 10 mmol) was added to the solution. The slow diffusion of Et_2O to the solution at room temperature yielded yellow crystals suitable for the X-ray analysis (127 mg, 83%). Anal. Calcd for $[K(C_{12}H_{24}O_6)]_4[HSiV_2W_{10}O_{39}(OCH_3)]\cdot 1.5CH_3CN$: C, 16.1; H, 2.71; N, 0.72. Found: C, 15.9; H, 2.69; N, 0.66. IR (KBr, cm^{-1}): 1106, 994, 965, 903, 872, 792, 702, 556, 409. ^{51}V NMR (CH_3CN): δ −548. ^{1}H NMR (CD_3CN containing 1% MeOH): δ 5.18 (1H, s, V−O*H*-V), 4.44 (3H, s, V−OC*H*$_3$−V), 3.58 (cation).

Synthesis of $[(CH_3)_4N]_4[\gamma\text{-}SiV_2W_{10}O_{38}(\mu\text{-}OCH_3)_2]\cdot 4CH_3CN$ (TMA−III). TMA−**I**[11] (180 mg, 60 μmol) was dissolved in DMSO/methanol (3 mL/ 0.3 mL), and tetramethylammonium hydroxide (25% aq, 22 μL, 60 μmol) was added. The solution was stirred for 1 h in the presence of the drying reagent (3 Å molecular sieves), and methyl iodide (12.4 μL, 200 μmol) was added. The solution was gently stirred overnight in the dark. Then the solution was filtered, and diethyl ether (20 mL) was added to the clear orange solution. After the mixture was left to stand for 15 min, the upper layer was removed by decantation, followed by the addition of water (5 mL). The resulting yellow precipitate was collected, washed with methanol, and recrystallized from acetonitrile. Yield: 75 mg (40%). ^{1}H NMR (D_2O): δ 4.62 (6H, s, $-OCH_3$), 3.19 (48H, s, cation). ^{1}H NMR (CD_3CN): δ 4.40 (6H, s, $-OCH_3$), 3.13 (48H, s, cation). ^{51}V NMR (CH_3CN): δ −535. IR (KBr, cm^{-1}): 997, 969, 952sh, 908, 868, 785, 711, 557, 539, 410. Single crystals suitable for X-ray analysis were obtained by the slow evaporation of the acetonitrile solution at room temperature.

Synthesis of $[(CH_3)_4N]_4[\gamma\text{-}HSiV_2W_{10}O_{39}(\mu\text{-}OC_2H_5)]$ (TMA−IV). TMA−**I**[11] (20 mg, 6.8 μmol) was dissolved in DMF (0.5 mL). Ethanol (3 mL) was carefully layered over the solution. The mixture stood in the dark for several days resulting in growth of yellow crystals suitable for X-ray crystallography. Yield: 88%. IR (KBr, cm^{-1}): 1101, 971, 950sh, 907, 870, 786, 705, 555, 455, 409. ^{51}V NMR (CH_3CN): δ −550. ^{1}H NMR (CD_3CN): δ 4.54 (2H, m, OC*H*$_2$−), 1.77 (3H, t, −C*H*$_3$), 3.15 (cation).

Esterification of I. TBA−**I** (54 mg, 15 μmol), H_2O (50−200 μL, 2.8−11.1 mmol), and methanol (10−40 μL, 0.25−1 mmol) were dissolved in CH_3CN (3 mL), and the reaction was traced by ^{51}V NMR spectroscopy at 298 ± 0.2 K. The spectra were recorded every 5 min until no changes were observed in the signal intensities. The spectra showed two signals at −564 and −549 ppm which were assigned to TBA−**I** and the methyl ester, respectively. The signal intensities reached constant values after 5 min. When the methyl ester (CEK−**II**) was hydrated in the same manner as used for the esterification of TBA−**I**, the signal intensities for **I** and **II** reached the same values as those in the esterification of TBA−**I**. The *K* value was unchanged when the order in which the TBA−**I**, water, and methanol were added was changed. These facts show that the effective equilibrium was achieved within 5 min. Esterification of the other alcohols with **I** was conducted according to the same procedure as that for the esterification of methanol, and the effective equilibrium was achieved within 25 min in each case.

Formoxylation of I. TBA−**I** (54 mg, 15 μmol), formic acid (100 μL, 2.65 mmol), and H_2O (2.5−10 μL, 0.14−0.57 mmol) were dissolved in CH_3CN (3 mL), and the reaction was traced by ^{51}V NMR spectroscopy at 298 ± 0.2 K. The formoxylated polyoxometalate **V** showed a ^{51}V NMR signal at −556 ppm. The effective equilibrium was achieved within 5 min.

Single crystals of **V** were obtained as follows. The tetraethylammonium salt of **I** (TEA−**I**) was synthesized using tetraethylammonium bromide according to the same procedure as that used

---

[12] Cold-spray ionization mass spectroscopy (CSI-MS) is a powerful method for the characterization of supramolecules with weak interactions: Yamaguchi, K. *J. Mass Spectrosc.* **2003**, *38*, 473. First application to polyoxometalate: Nakagawa, Y.; Kamata, K.; Kotani, M.; Yamaguchi, K.; Mizuno, N. *Angew. Chem., Int. Ed.* **2005**, *44*, 5136.

[13] Canny, J.; Thouvenot, R.; Tézé, A.; Hervé, G.; Leparulo-Loftus, M.; Pope, M. T. *Inorg. Chem.* **1991**, *30*, 976.

[14] Tézé, A.; Hervé, G. *Inorg. Synth.* **1990**, *27*, 85.

[15] Tézé, A.; Canny, J.; Gurdan, L.; Thouvenot, R.; Hervé, G. *Inorg. Chem.* **1996**, *35*, 1001.

Table 1. Crystallographic Data for CEK−**II**, TMA−**III**, TMA−**IV**, and TEA−**V**

	CEK−**II**	TMA−**III**	TMA−**IV**	TEA−**V**
formula	$[K(C_{12}H_{24}O_6)]_4$ $[HSiV_2W_{10}O_{39}(OCH_3)]$ $\cdot 1.5CH_3CN$	$[N(CH_3)_4]_4$ $[SiV_2W_{10}O_{38}(OCH_3)_2]$ $\cdot 4CH_3CN$	$[N(CH_3)_4]_4$ $[HSiV_2W_{10}O_{39}(OC_2H_5)]$ $\cdot 2.5(CH_3)_2NCHO$	$[N(C_2H_5)_4]_4$ $[HSiV_2W_{10}O_{39}(OOCH)]$ $\cdot 2C_4H_8O_2$
fw	3814.06	3099.31	3116.82	3335.69
cryst syst	triclinic	monoclinic	triclinic	triclinic
space group	$P\bar{1}$	$P2_1/m$	$P\bar{1}$	$P\bar{1}$
a (Å)	15.107(7)	11.5707(3)	13.1578(2)	14.035(4)
b (Å)	17.440(8)	22.2153(6)	13.5146(3)	14.666(4)
c (Å)	21.742(12)	13.3566(3)	21.2057(4)	19.784(5)
α (deg)	81.44(2)	90	77.7050(8)	77.660(9)
β (deg)	84.21(2)	113.371(2)	89.5480(8)	80.364(9)
γ (deg)	67.64(2)	90	81.9440(13)	87.810(10)
V (Å^3)	5232.6(43)	3151.6(1)	3647.06(12)	3922.1(19)
Z	2	2	2	2
T (K)	183	153	153	103
wavelength (Å)	0.71070	0.71070	0.71070	0.71070
D_{calcd} (g cm^{-3})	2.421	3.266	2.838	2.824
abs coeff (cm^{-1})	113.67	185.84	160.62	149.47
no. of reflns	21485	8440	18436	9008
no. of observations	10511	5675	13185	7819
R^a	0.064	0.039	0.039	0.070
$R_w{}^a$	0.072	0.059	0.052	0.087

^{a} $R = \sum||F_o| - |F_c||/\sum|F_o|$. $R_w = [\sum w(|F_o| - |F_c|)^2/\sum w(F_o)^2]^{1/2}$. $I > 3\sigma(I)$.

for TBA−**I** and recrystallized from acetonitrile (yield, 85%). TEA−**I** (10 mg, 3.2 μmol) was dissolved in formic acid (1 mL), and 1,4-dioxane (3 mL) was carefully layered over the solution. The mixture was left standing for several days which yielded yellow prismatic crystals suitable for the X-ray analysis.

X-ray Crystallography. The crystals were mounted on a loop for indexing and intensity data collection at 103−183 K on a Rigaku Mercury CCD area detector (CEK−**II**) or Rigaku Saturn CCD area detector (TMA−**III**, TMA−**IV**, and TEA−**V**) with graphite monochromated Mo Kα radiation ($\lambda = 0.71070$ Å). The structures were solved by direct methods[16] (for TMA−**III** and TMA−**IV**) or by heavy-atom Patterson methods[17] (for CEK−**II** and TEA−**V**) and were expanded using Fourier techniques.[18] The crystal parameters are summarized in Table 1. All calculations were performed using the CrystalStructure crystallographic software package.[19]

Quantum Chemical Calculations. The calculations were carried out at the B3LYP[20] level of theory with 6-31++G** basis sets for H, C, and O atoms, 6-31G* for Si atoms, and the double-ζ quality basis sets with effective core potentials proposed by Hay and Wadt[21] for V and W atoms. The formation energies (ΔE) of methyl ester were expressed by $\Delta E = E(\text{methyl ester}) + E(H_2O) - E(\text{protonated polyoxometalate}) - E(CH_3OH)$. The geometries were optimized within the following symmetry restrictions: C_{2v} for H_2O and $[\gamma\text{-}H_2SiV_2W_{10}O_{40}]^{4-}$ and C_s for CH_3OH, $[\gamma\text{-}HSiV_2W_{10}O_{39}(OCH_3)]^{4-}$, $[\beta\text{-}HSiV_3W_9O_{40}]^{6-}$, and $[\beta\text{-}SiV_3W_9O_{39}(OCH_3)]^{6-}$. All calculations were performed with the Gaussian03 program package.[22]

Results and Discussion

Reaction with Alcohols. The methyl monoester of **I** (**II**) was easily formed by the addition of methanol to the acetonitrile solution of **I**. The formation of **II** was highly selective. The dimethyl ester of **I** (**III**) was not formed by the reaction of **I,** even with excess methanol in acetonitrile for one week, but **III** was synthesized by the reaction of **II** with methyl iodide.[23] The esterification reaction was reversible and the hydrolysis of **II** readily proceeded in the presence of water. The single crystals of **II** were obtained by vapor diffusion of diethyl ether into the acetonitrile solution of the 18-crown-6-potassium salt derivative of **I** (CEK−**I**) containing methanol. As shown in Figure 1, anionic cluster **II** retained the γ-Keggin structure, and the two vanadium atoms were bridged with one oxygen atom and one methoxo group. The bond valence sum (BVS) value of O2 was 1.16 and was clearly different from those of the other oxygen atoms (1.53−2.10), indicating that the oxygen atom remained protonated.[24] The ^{1}H NMR spectrum of CEK−**II** in CD_3CN showed two lines at 4.44 (sharp, 3H per anion) and 5.18 ppm (broad, 1H per anion), in addition to the lines assigned to the solvent and countercation.

The ethyl monoester of **I** (**IV**) was also formed by the addition of ethanol to the DMF solution of **I**. As shown in

---

(16) SIR92. Altomare, A.; Burla. M.C.; Camalli, M.; Cascarano, G.; Giacovazzo, C.; Guagliardi, A.; Polidori, G. *J. Appl. Cryst.* **1994**, *27*, 435.

(17) Beuskens, P. T.; Admiraal, G.; Beurskens, G.; Bosman, W. P.; Garcia-Granda, S.; Gould, R. O.; Smits, J. M. M.; Smykalia, C. *PATTY*; Crystallography Laboratory, University of Nijmegen: The Netherlands,-1992.

(18) Beuskens, P. T.; Admiraal, G.; Beurskens, G.; Bosman, W. P.; de Gelder, R.; Israel, R.; Smits, J. M. M. *DIRDIF99*; Crystallography Laboratory, University of Nijmegen: The Netherlands, 1999.

(19) *CrystalStructure 3.6.0*; Rigaku/MSC: Tokyo, Japan, 2004.

(20) Becke, A. D. *J. Chem. Phys.* **1993**, *98*, 1372.

(21) Hay, P. J.; Wadt, W. R. *J. Chem. Phys.* **1985**, *82*, 270.

(22) Frisch, M. J.; Trucks, G. W.; Schlegel, H. B.; Scuseria, G. E.; Robb, M. A.; Cheeseman, J. R.; Montgomery, J. A., Jr.; Vreven, T.; Kudin, K. N.; Burant, J. C.; Millam, J. M.; Iyengar, S. S.; Tomasi, J.; Barone, V.; Mennucci, B.; Cossi, M.; Scalmani, G.; Rega, N.; Petersson, G. A.; Nakatsuji, H.; Hada, M.; Ehara, M.; Toyota, K.; Fukuda, R.; Hasegawa, J.; Ishida, M.; Nakajima, T.; Honda, Y.; Kitao, O.; Nakai, H.; Klene, M.; Li, X.; Knox, J. E.; Hratchian, H. P.; Cross, J. B.; Bakken, V.; Adamo, C.; Jaramillo, J.; Gomperts, R.; Stratmann, R. E.; Yazyev, O.; Austin, A. J.; Cammi, R.; Pomelli, C.; Ochterski, J. W.; Ayala, P. Y.; Morokuma, K.; Voth, G. A.; Salvador, P.; Dannenberg, J. J.; Zakrzewski, V. G.; Dapprich, S.; Daniels, A. D.; Strain, M. C.; Farkas, O.; Malick, D. K.; Rabuck, A. D.; Raghavachari, K.; Foresman, J. B.; Ortiz, J. V.; Cui, Q.; Baboul, A. G.; Clifford, S.; Cioslowski, J.; Stefanov, B. B.; Liu, G.; Liashenko, A.; Piskorz, P.; Komaromi, I.; Martin, R. L.; Fox, D. J.; Keith, T.; Al-Laham, M. A.; Peng, C. Y.; Nanayakkara, A.; Challacombe, M.; Gill, P. M. W.; Johnson, B.; Chen, W.; Wong, M. W.; Gonzalez, C.; Pople, J. A. *Gaussian 03*, revision B.03; Gaussian, Inc.: Wallingford, CT, 2004.

(23) **I** was quickly converted to the monomethyl ester **II** in DMSO/MeOH (the reaction solvent), which was confirmed by ^{1}H and ^{51}V NMR spectra (4.33 and −548 ppm, respectively).

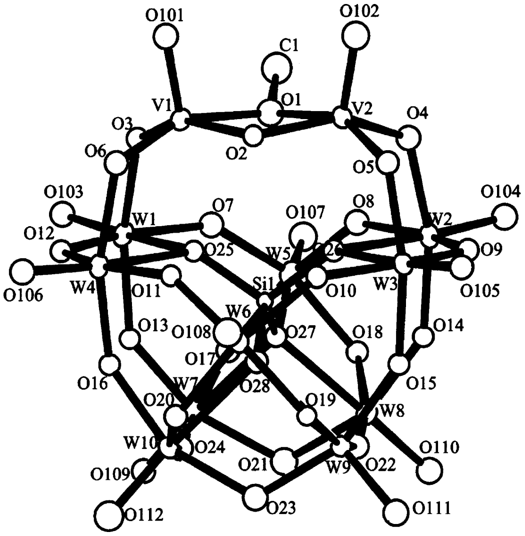

Figure 1. ORTEP view of CEK−**II**. For clarity, 18-crown-6-potassium cations and solvent molecules are omitted. Selected lengths (Å): O1−C1, 1.46(4); V1−O1, 1.98(2), V1−O2, 2.00(2); V2−O1, 1.96(3); V2−O2, 2.01-(1); V1−V2, 3.155(7).

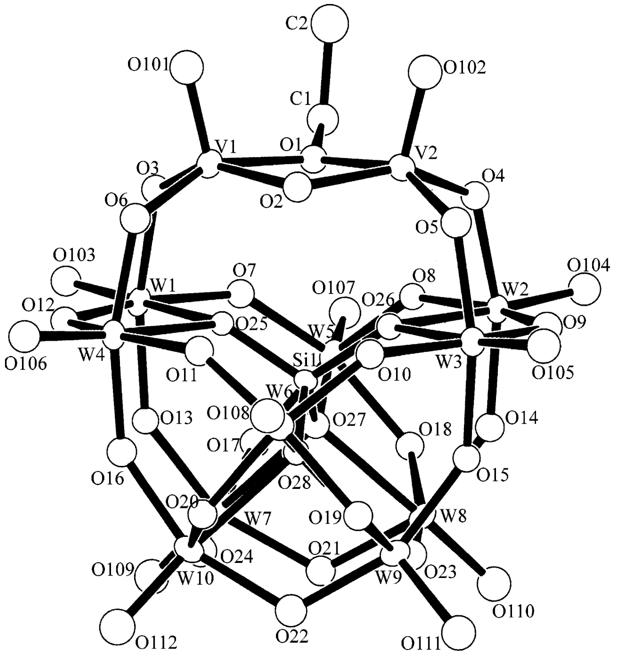

Figure 2. ORTEP view of TMA−**IV**. For clarity, tetramethylammonoium cations and solvent molecules are omitted. Selected lengths (Å): C1−C2, 1.52(2); O1−C2, 1.470(19); V1−O1, 1.958(10); V1−O2, 1.944(10); V2−O1, 1.969(10); V2−O2, 1.949(10); V1−V2, 3.128(3).

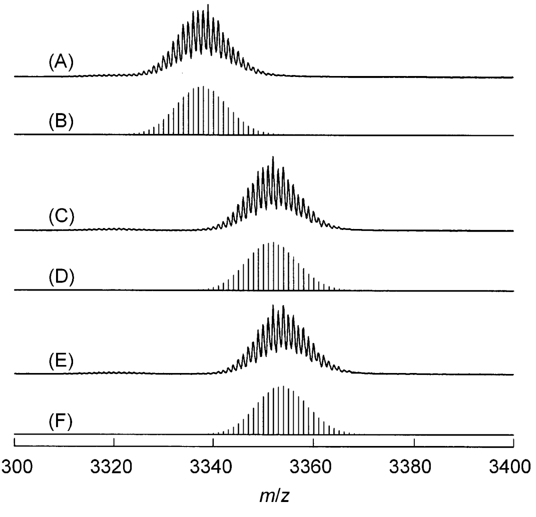

Figure 3. CSI-MS spectra of TBA−**I** and TBA−**II** in MeCN at 293 K: (A) TBA−**I**, 0.14 mM; (B) calculated pattern of $[(TBA)_3H_2SiV_2W_{10}O_{40}]^-$; (C) TBA−**I**, 0.14 mM, MeOH, 25 mM; (D) calculated pattern of $[(TBA)_3HSiV_2W_{10}O_{39}(OCH_3)]^-$; (E) TBA−**I**, 0.14 mM, $Me^{18}OH$, 25 mM; and (F) calculated pattern of $[(TBA)_3HSiV_2W_{10}O_{39}(^{18}OCH_3)]^-$.

Figure 2, anionic cluster **IV** also retained the γ-Keggin structure. The two vanadium atoms were bridged with one oxygen atom (O2) and one ethoxo group. The BVS value of O2 was 1.36 and was clearly different from those of the other oxygen atoms (1.73−2.10), indicating that the oxygen atom remained protonated.[25]

The cold-spray ionization mass (CSI-MS, anion mode) spectrum of the tetrabutylammonium salt of **I** (TBA−**I**) in MeCN showed the most intense parent ion peaks centered at *m*/*z* 3338 with the isotopic distribution (Figures 3A and S1), which agreed with the calculated pattern of $[(TBA)_3H_2SiV_2W_{10}O_{40}]^-$ (Figure 3B). Upon the addition of 180 equiv of MeOH with respect to **I**, new peaks centered at *m*/*z* 3352, which agreed with the calculated pattern of $[(TBA)_3HSiV_2W_{10}O_{39}(OCH_3)]^-$ (Figure 3D), appeared (Figure 3C), while the peaks centered at *m*/*z* 3338 disappeared. Upon the addition of $Me^{18}OH$ instead of $Me^{16}OH$, peaks centered at *m*/*z* 3354 appeared (Figure 3E). The ^1H NMR spectrum of **I** (1 mM) in CD_3CN showed a signal at 5.06 ppm from the hydroxyl proton of the $\{VO-(\mu\text{-}OH)_2-VO\}$ core in **I**. Upon addition of 10 equiv of MeOH with respect to **I**, one signal appeared at 4.43 ppm, and the 5.06-ppm signal was weakened by ca. 50% and shifted to 5.13 ppm. One new ^{51}V NMR signal appeared at −549 ppm in MeCN upon addition of 10 equiv of MeOH, and the −564 ppm signal of the $\{VO-(\mu\text{-}OH)_2-VO\}$ core in **I** disappeared. Six new ^{183}W NMR signals appeared at −80.9, −93.3, −94.5, −122.8, −124.8, and −134.9 ppm with intensities of 2(br)/1/2(br)/1/2/2, respectively, upon the addition of 10 equiv of MeOH, and the signals at −82.2, −95.6, and −129.1 ppm for **I** disappeared. One ^{13}C NMR signal appeared at 69 ppm (1C per anion), the value of which falls in the range of those

---

(24) BVS values of atoms in CEK−**II** (atom, BVS): V1, 4.85; V2, 4.95; W1, 5.66; W2, 5.81; W3, 5.95; W4, 5.80; W5, 5.96; W6, 5.73; W7, 5.66; W8, 5.70; W9, 5.82; W10, 5.69; Si, 3.70; O1, 2.10; O2, 1.16; O3, 1.90; O4, 1.80; O5, 1.90; O6, 1.80; O7, 1.94; O8, 1.86; O9, 1.85; O10, 1.94; O11, 1.85; O12, 1.91; O13, 1.86; O14, 1.91; O15, 1.93; O16, 1.91; O17, 1.91; O18, 1.94; O19, 1.88; O20, 1.93; O21, 1.78; O22, 1.98; O23, 1.85; O24, 1.96; O25, 1.72; O26, 1.71; O27, 1.87; O28, 1.86; O101, 1.68; O102, 1.83; O103, 1.66; O104, 1.70; O105, 1.61; O106, 1.66; O107, 1.75; O108, 1.75; O109, 1.57; O110, 1.53; O111, 1.66; O112, 1.74.

(25) BVS values of atoms in TMA−**IV** (atom, BVS): V1, 5.17; V2, 5.21; W1, 6.09; W2, 6.09; W3, 6.10; W4, 6.16; W5, 6.25; W6, 6.24; W7, 6.13; W8, 6.20; W9, 6.16; W10, 6.12; Si, 3.89; O1, 2.10; O2, 1.36; O3, 1.98; O4, 1.95; O5, 1.96; O6, 2.03; O7, 2.02; O8, 2.04; O9, 1.94; O10, 2.05; O11, 2.03; O12, 1.95; O13, 2.02; O14, 2.01; O15, 2.01; O16, 2.02; O17, 1.98; O18, 1.99; O19, 1.97; O20, 1.96; O21, 1.92; O22, 1.97; O23, 2.10; O24, 2.10; O25, 1.90; O26, 1.90; O27, 1.95; O28, 1.93; O101, 1.82; O102, 1.85; O103, 1.73; O104, 1.75; O105, 1.80; O106, 1.76; O107, 1.85; O108, 1.77; O109, 1.75; O110, 1.82; O111, 1.79; O112, 1.78.

Table 2. Dehydrative Condensation Reaction of **I** with Various Alcohols and Acids in Acetonitrile at 298 K

hydroxo compound	observed (calcd) mol wt of $[(\mathrm{TBA})_3(\mathrm{ester})]^-$	$\delta(^{51}\mathrm{V})$ of ester	$\delta(^{1}\mathrm{H})$ of ester	K[a]	pK_a
methanol	3352.2 (3351.9)	−549	5.13(1H,br) 4.43(3H,s)	75 ± 5	15.1[b]
ethanol	3366.6 (3365.9)	−550	5.01(1H,br) 4.54(2H,br) 1.77(3H,t)	20 ± 2	15.9[b]
1-propanol	3380.4 (3379.9)	−547	5.03(1H,br) 4.38(2H,br) 2.37(2H,q) 1.03(3H,t)	9.5 ± 0.5	16.1[b]
2-propanol	3380.1 (3379.9)	−552	5.10(1H,br) 3.8−4.2[e] 1.69(6H,d)	<0.01	16.6[c]
1-butanol	3394.5 (3394.0)	−547	5.02(1H,br) 4.44(2H,br) 2.31(2H,t) 1.53(2H,m) 1.02(3H,t)	9.7 ± 0.9	16.1[b]
2-methyl-1-propanol	3394.5 (3394.0)	−538	5.05(1H,br) 4.31(2H,d) 2.90(1H,m) 1.15(6H,d)	1.0 ± 0.1	16.1[b]
2,2-dimethyl-1-propanol	3408.3 (3408.0)	−540	5.18(1H,br) 4.39(2H,s) 1.33(9H,s)	0.016 ± 0.002	no data reported
tert-butyl alcohol	−[d] (3408.0)	−[d]	−	0	16.9[c]
benzyl alcohol	3428.6 (3428.0)	−544	7.73(2H,d) 7.2−7.4[e] 5.44(2H,s) 5.00(1H,s)	5.5 ± 0.2	15.4[c]
4-methylbenzyl alcohol	3442.5 (3442.0)	−544	7.83(2H,d) 7.1−7.3[e] 5.39(2H,s) 5.04(1H,br) 2.3[e]	6.7 ± 0.2	15.6[c]
4-methoxybenzyl alcohol	3458.8 (3458.0)	−544	7.87(2H,m) 6.9−7.3[e] 5.38(2H,s) 5.05(1H,br) 3.8[e]	8.9 ± 0.3	15.6[c]
4-fluorobenzyl alcohol	3446.7 (3446.0)	−544	7.96(2H,m) 7.0−7.4[e] 5.42(2H,s) 5.02(1H,br)	9.3 ± 0.3	15.4[c]
4-chlorobenzyl alcohol	3463.1 (3462.4)	−544	7.93(2H,m) 7.3−7.4[e] 5.41(2H,s) 5.03(1H,br)	8.9 ± 0.5	15.3[c]
4-nitrobenzyl alcohol	3473.4 (3473.0)	−542	8.1−8.2[e] 7.5−7.6[e] 5.54(2H,s) 5.09(1H,br)	9.5 ± 0.5	14.9[c]
formic acid	3366.0 (3365.9)	−556	8.59(1H,s)	0.06 ± 0.02	3.75
acetic acid	−[d] (3379.9)	−[d]	−	0	4.56

[a] $K = ([\mathrm{ester}][\mathrm{H_2O}])/([\mathrm{I}][\mathrm{alcohol}])$. [b] Murto, J. *Acta Chem. Scand.* **1964**, *18*, 1043. [c] Brink, H. *Acta Pharm. Suec.* **1980**, *17*, 233. [d] No ester was observed. [e] Overlapped with the signals of the parent alcohol.

reported for diamagnetic metal methoxides.[26] These CSI-MS and NMR data show the in situ formation of monoester species of {VO−(μ-OH)(μ-OCH$_3$)-VO} according to eq 1.

$$\gamma\text{-H}_2\text{SiV}_2\text{W}_{10}\text{O}_{40}{}^{4-}\ (\mathbf{I}) + \text{CH}_3{}^*\text{OH} \rightarrow \gamma\text{-HSiV}_2\text{W}_{10}\text{O}_{39}(\mu\text{-}{}^*\text{OCH}_3)^{4-}\ (\mathbf{II}) + \text{H}_2\text{O} \quad (1)$$

The esterification reaction was reversible, and the hydrolysis of **II** readily proceeded in the presence of water. The formation constants (K) of the ester ($K = \{[\mathbf{II}][\mathrm{H_2O}]\}/\{[\mathbf{I}][\mathrm{MeOH}]\}$) in water (buffered with 0.1 M $\mathrm{NaHSO_4}$/0.1 M $\mathrm{Na_2SO_4}$, pH = 1.67) and acetonitrile at 298 K were determined to be 75 ± 2 and 75 ± 5, respectively, by ^{51}V NMR spectroscopy. These values are much larger than those reported for methyl monovanadate ($\mathrm{H_2VO_{4-}}$ + MeOH, $K_1 = 5.2 \pm 0.1$, $K_2 = 1.2 \pm 0.1$),[27] methyl divanadate ($(\mathrm{HO})\mathrm{O_2VOVO_2(OH)}^{2-}$ + MeOH, $K_1 = 3.0 \pm 0.3$, $K_2 = 3.1 \pm 0.3$),[27] methyl ester of Dawson-type trivanadium-substituted phosphotungstate ($\mathrm{HP_2V_3W_{15}O_{59}}(\mu\text{-OH})_3{}^{5-}$ + MeOH, $K_1 = 2.0 \pm 0.2$, $K_2 = 1.3 \pm 0.2$, $K_3 = 0.37 \pm 0.08$),[28] methyl acetate (5.9 ± 0.2),[29] and monoethyl phosphate (K_1

---

(26) Farneth, W. E.; Staley, R. H.; Domaille, P. J.; Farlee, R. D. *J. Am. Chem. Soc.* **1987**, *109*, 4018.

(27) Tracey, A. S.; Gresser, M. J.; Galeffi, B. *Inorg. Chem.* **1988**, *27*, 157.

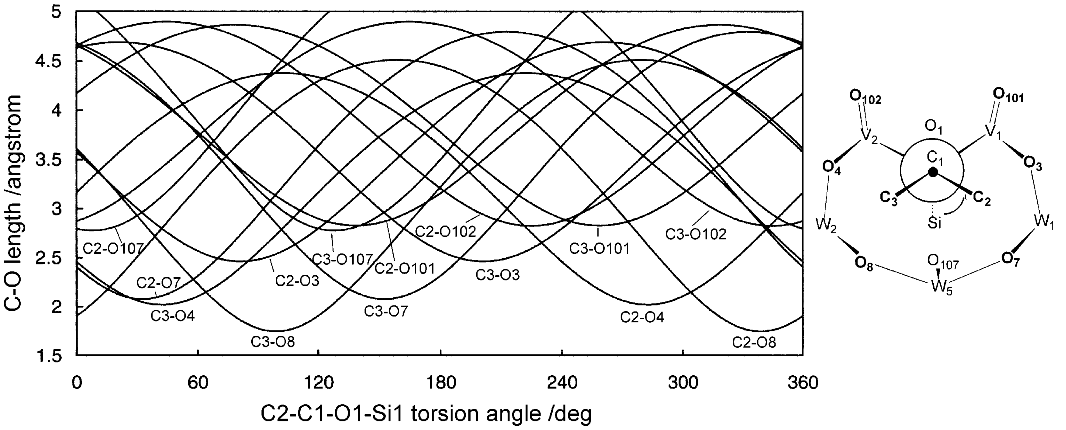

Figure 4. Distances between methyl groups and polyoxometalate atoms in the model structure for the isopropyl ester of **I**.

= 0.46).[30] Unlike $HP_2V_3W_{15}O_{59}(\mu\text{-OH})_3{}^{5-}$ and **I**, β-Keggin-type tri-vanadium-substituted silicotungstate β-1,2,3-$H_xSiV_3W_9O_{40}{}^{(7-x)-}$ has been reported to be inactive for the esterification,[31] although V$-$(μ-OH)$-$V bridge is present in all three polyoxometalates. The order of reactivity of the bridging hydroxo groups with the vanadium-substituted polyoxotungstates decreased in the following order: **I** > $H_4P_2V_3W_{15}O_{62}{}^{5-}$ > β-1,2,3-$H_xSiV_3W_9O_{40}{}^{(7-x)-}$. The order of the formation constants can possibly be explained by the difference of the V$-$OR$-$V bond angles. The V$-$OR$-$V bond angle in **II** (106°) is closer to the ideal angle for the sp^3 electronic state (109°) than that in β-1,2,3-$H_xSiV_3W_9O_{40}{}^{(7-x)-}$ (150°).[32] The sp^3-like character of the V$-$OMe$-$V oxygen atom in **II** would stabilize the ester. This idea was supported by the following calculation: the formation energies (ΔE) of methyl ester were calculated with B3LYP density functional[20] to be +2.6 kJ mol^{-1} and +30.4 kJ mol^{-1} for γ-$HSiV_2W_{10}O_{39}(OMe)^{4-}$ and β-1,2,3-$SiV_3W_9O_{39}(OMe)^{6-}$, respectively, where ΔE was expressed by $\Delta E = E(\mathbf{II}) + E(H_2O) - E(\mathbf{I}) - E(\text{MeOH})$. By using these ΔE values in combination with the formation constant of γ-$HSiV_2W_{10}O_{39}(OMe)^{4-}$, the formation constant of β-1,2,3-$SiV_3W_9O_{39}(OMe)^{6-}$ is calculated to be $1.0 \times 10-^{3}$,[33] which is in agreement with the fact that $H_xSiV_3W_9O_{40}{}^{(7-x)-}$ was inactive for the esterification.

The esterification of **I** with various alcohols was investigated, and the results are summarized in Table 2. Only monoesters were observed, and no diester was observed for all alcohols. The *K* values decreased in the order of methanol > ethanol > 1-propanol ≈ 1-butanol and primary alcohols ≫ secondary alcohols ≥ tertiary alcohols = 0, and those for secondary and tertiary alcohols were much smaller than those for monovanadate esters (K_1 = 5.0 (2-propanol); 3.4 (*tert*-butyl alcohol)).[9] Such smaller *K* values observed for secondary and tertiary alcohols are probably caused by the steric crowding resulting from introduction of secondary carbon center at the bridging oxygen site. The *K* values for para-substituted benzyl alcohols were smaller than that of ethanol, while the pK_a values for para-substituted benzyl alcohols (14.89$-$15.64) are smaller than that of ethanol (15.9),[34] which is consistent with the idea. It has also been reported that ester formation of secondary and tertiary alcohols on the Nb$-$O$-$Nb bridging site in $Nb_2W_4O_{19}{}^{4-}$ is prevented by the steric crowding between the alcohols and the polyoxometalate framework.[35] Figure 4 shows the structural model for isopropyl ester constructed by the addition of two methyl groups to the carbon center of **II**. In every C2$-$C1$-$O1$-$Si1 torsion angle, the minimum length of Cx$-$Oy (x = 2, 3; y = 3, 4, 7, 8, 101, 102) was shorter than the sum of van der Waals radius of a C atom (1.70 Å) and the ion radius of O^{2-} (1.22 Å); therefore, the steric crowding between the methyl groups and the polyoxometalate framework results in much smaller *K* values for isopropyl and *tert*-butyl esters.

Reaction with Carboxylic Acids. TBA$-$**I** also reacted with formic acid to form polyoxotungstovanadium formate (**V**). Single crystals of **V** were successfully obtained as a tetraethylammonium salt derivative from the HCOOH/1,4-dioxane solution of **I**. As shown in Figure 5, anionic cluster **V** retained the γ-Keggin structure, and four tetraethylammonium cations per **V** existed. The two vanadium atoms were bridged with one hydroxo group and one formate ligand (O1$-$C1$-$O100); the BVS value of O2 was calculated to be 1.27 and was clearly different from those of the other oxygen atoms (1.64$-$2.31),[36] indicating that the oxygen atom remained protonated. The V$-$O1 lengths were 2.03(3) (V1$-$O1) and 2.05(5) Å (V2$-$O1), indicating that these two bonds are almost equivalent. The O1$-$C1 and C1$-$O100 lengths were 1.32(6) and 1.16(7) Å, respectively. The respective values are close to those (C$-$OH, 1.343; C═O, 1.202 Å)[37] of formic acid and different from that of sodium formate

---

[28] (a) Zeng, H.; Newkome, G. R.; Hill, C. L. *Angew. Chem., Int. Ed.* **2000**, *39*, 1771. (b) Hou, Y.; Hill, C. L. *J. Am. Chem. Soc.* **1993**, *115*, 11823.

[29] Lee, D. G.; Yan, Y.; Changler, W. D. *Anal. Chem.* **1994**, *66*, 32.

[30] Bourne, N.; Williams, A. *J. Org. Chem.* **1984**, *49*, 1200.

[31] Finke, R. G.; Rapko, B.; Saxton, R. J.; Domaille, P. J. *J. Am. Chem. Soc.* **1986**, *108*, 2947.

[32] Tézé, A.; Cadot, E.; Béreau, V.; Hervé, G. *Inorg. Chem.* **2001**, *40*, 2000.

[33] The formation reaction of β-1,2,3-$SiV_3W_9O_{39}(OMe)^{6-}$ and γ-$HSiV_2W_{10}O_{39}(OMe)^{4-}$ would have similar ΔS values because the molecules used in the reactions are similar to each other. Therefore, we calculated the formation constant (*K*) assuming that the ΔS values for the reactions were equal to each other.

[34] (a) Brink, H. *Acta Pharm. Suec.* **1980**, *17*, 233. (b) Murto, J. *Acta Chem. Scand.* **1964**, *18*, 1043.

[35] Day, V. W.; Klemperer, W. G.; Schwartz, C. *J. Am. Chem. Soc.* **1987**, *109*, 6030.

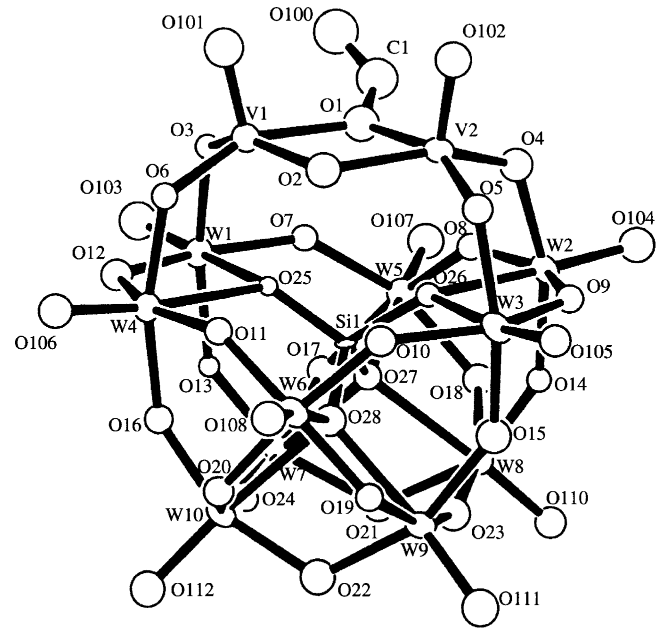

Figure 5. ORTEP view of TEA−**V**. For clarity, tetraethylammonium cations and solvent molecules are omitted. Selected lengths (Å): C1−O100, 1.16(7); C1−O1, 1.32(6); V1−O1, 2.03(3); V1−O2, 1.96(3); V2−O1, 2.05(3); V2−O2, 1.98(3); V1−V2, 3.26(1).

(1.27 Å).[38] Neither metal atoms nor hydrogen-donor molecules, such as formic acid, were found around O100. This coordination mode of the carboxylate ligand to vanadium is novel in contrast to the usual symmetrical syn−syn coordination of the carboxylate bridge.[39]

Figure 6 shows the CSI-MS spectrum of TBA−**I**. Upon addition of formic acid, new peaks centered at *m/z* 3338 + 28, which agreed with the calculated pattern of $[(TBA)_3HSiV_2W_{10}O_{39}(OOCH)]^-$, appeared (Figure 6C and D). The ^{51}V NMR spectrum showed a line at −556 ppm in addition to the line of **I**. The formate derivative of **I** (**V**) was very sensitive to water. The formation constant (*K*) of **V** ($K = \{[\mathbf{V}][H_2O]\}/\{[\mathbf{I}][HCOOH]\}$) in MeCN at 298 K was determined to be 0.06 ± 0.02 by ^{51}V NMR. The basicity of the formate ion (pK_a of the conjugate acid (HCOOH): 3.75)[40] is weaker than that of alcoholate ions (pK_a of the conjugate acids (alcohols): ∼16). Since the vanadium(V) centers work as Lewis acids, they would favor more basic ligands of alcoholates, which would explain the difference in the formation constants between **V** and **II**.

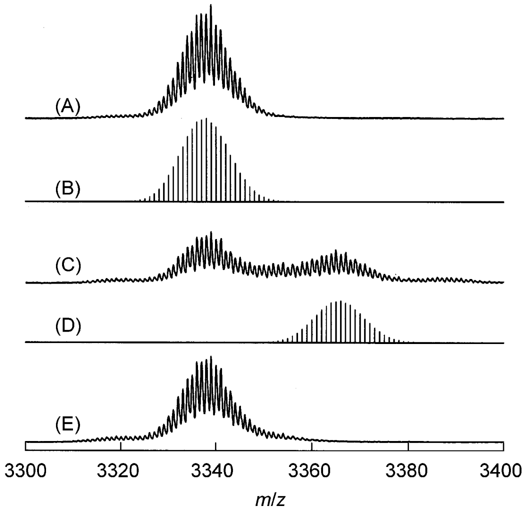

Figure 6. CSI-MS spectra of TBA−**I** in the presence of carboxylic acid (solvent, MeCN, 293 K): (A) TBA−**I**, 0.14 mM, (B) calculated pattern of $[(TBA)_3H_2SiV_2W_{10}O_{40}]^-$; (C) TBA−**I**, 0.14 mM, H_2O, 56 mM, HCOOH, 0.53 M; (D) calculated pattern of $[(TBA)_3H_2SiV_2W_{10}O_{39}(OOCH)]^-$; and (E) TBA−**I**, 0.14 mM, H_2O, 56 mM, CH_3COOH, 0.35 M.

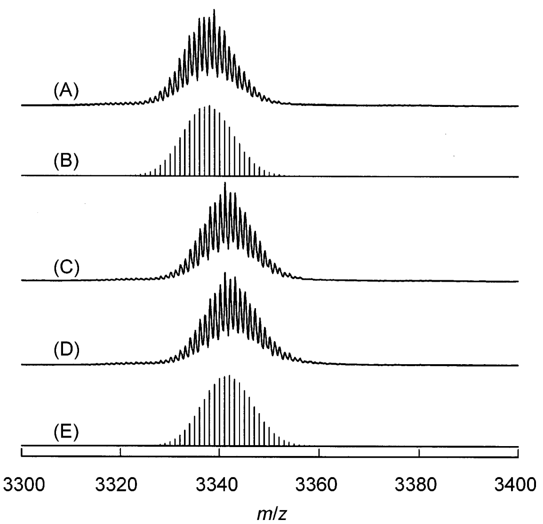

Figure 7. CSI-MS spectra of TBA−**I** (solvent, MeCN, 293 K): (A) TBA−**I**, 0.14 mM; (B) calculated pattern of $[(TBA)_3H_2SiV_2W_{10}O_{40}]^-$; (C) 5 min after $H_2{}^{18}O$ (56 mM) was added to the mixture in spectrum A; (D) 1 h after $H_2{}^{18}O$ was added to the mixture in spectrum A; and (E) calculated pattern of $[(TBA)_3SiV_2W_{10}O_{38}(^{18}OH)_2]^-$.

CSI-MS (Figure 6E) and ^{51}V NMR spectra were not changed by the addition of acetic acid to an MeCN solution of **I**, showing that **I** does not react with acetic acid despite it having weaker acidity than formic acid. This would also be explained by the steric crowding between the acetate ligand and the polyoxometalate framework. When the structural model of the acetate derivative of **I** was constructed by the addition of secondary carbon center (C2) to the C1 atom in Figure 5, the lengths of C2−O4 and C2−O8 became 2.70 and 2.74 Å, respectively. These values are much smaller than the sum (2.92 Å) of the van der Waals radius of the C atom and the ion radius of O^{2-}, supporting the steric crowding between the acetate ligand and the polyoxometalate framework.

Oxygen Exchange of I with H_2O. The reaction of TBA−**I** with $H_2{}^{18}O$ in MeCN was monitored with CSI-MS (Figure

---

(36) BVS values of atoms in TEA−**V** (atom, BVS): V1, 5.08; V2, 5.22; W1, 6.24; W2, 6.16; W3, 6.15; W4, 6.01; W5, 6.28; W6, 6.25; W7, 6.44; W8, 6.04; W9, 6.04; W10, 6.42; Si1, 3.98; O1, 2.26; O2, 1.27; O3, 1.82; O4, 2.00; O5, 2.05; O6, 1.93; O7, 2.04; O8, 2.03; O9, 2.31; O10, 1.97; O11, 1.91; O12, 1.99; O13, 2.08; O14, 2.01; O15, 1.97; O16, 2.07; O17, 1.76; O18, 2.07; O19, 2.04; O20, 2.18; O21, 2.03; O22, 2.08; O23, 1.94; O24, 2.11; O25, 1.93; O26, 1.76; O27, 2.00; O28, 1.91; O101, 1.93; O102, 1.64; O103, 1.95; O104, 1.85; O105, 1.90; O106, 1.85; O107, 1.90; O108, 1.75; O109, 1.66; O110, 2.06; O111, 1.85; O112, 1.70.

(37) *CRC Handbook of Chemistry and Physics*, 82nd ed.; CRC Press LLC: Boca Raton, 2001; pp 9−26.

(38) Zachariasen, W. H. *J. Am. Chem. Soc.* **1940**, *62*, 1011.

(39) (a) Gouzerh, P.; Proust, A. *Chem. Rev.* **1998**, *98*, 77. (b) Khan, M. I.; Zubieta, J. *Prog. Inorg. Chem.* **1995**, *43*, 1. (c) Cotton, F. A.; Wilkinson, G.; Murillo, C. A.; Bochmann, M. *Advanced Inorganic Chemistry*, 6th ed.; John Wiley & Sons: New York, 1999; p 486.

(40) *CRC Handbook of Chemistry and Physics*, 82nd ed.; CRC Press LLC: Boca Raton, 2001; pp 8−46.

7). The spectrum was not changed by the addition of $H_2{}^{16}O$ (0.05 vol %, 400 equiv). Upon the addition of 360 equiv (0.05 vol %) of $H_2{}^{18}O$, the peaks were shifted to the higher *m*/*z* numbers. After 5 min, peaks centered at *m*/*z* 3338 + 4 were observed, and they are in agreement with the calculated pattern of $[(TBA)_3H_2SiV_2W_{10}O_{38}{}^{18}O_2]^-$ (Figure 7C and E). The spectrum changed little after 1 h (Figure 7D). Upon the addition of $H_2{}^{18}O$ (12.5 equiv), the IR peaks at 843 and 699 cm^{-1} were shifted by -2 and -3 cm^{-1}, respectively, while the peaks at 1050−950 (M = O), 920−905 (Si−O), 876 (W−Oc−W), and 799 cm^{-1} (W−Oe−W, V−Oe−W)[41] were not shifted ($|\Delta\nu| < 1$ cm^{-1}) (Figure S8). Taking into account the C_{2v} symmetry of **I** and the fact that two oxygen atoms were exchanged, only the exchange of the V−(μ-*OH)$_2$−V site can explain the IR data. Upon the monomethylation of the V−(μ-OH)$_2$−V site in **I**, the bands of 843 and 699 cm^{-1} were shifted to 818 and 706 cm^{-1}, respectively, and the other bands between 1050 and 650 cm^{-1} were not shifted ($|\Delta\nu| < 2$ cm^{-1}), suggesting that these two bands are related to the V−(μ-OH)$_2$−V site. These results show that the V−(μ-OH)$_2$−V site in **I** easily exchanges oxygen atoms with water, while the exchange of the other oxygen atoms in **I** with water is very slow.[42]

Conclusions

The dehydrative condensation reaction of the bis-(μ-hydroxo) divanadium core in **I** with various hydroxo compounds of water, primary alcohols, and formic acid proceeds smoothly, and the crystal structures of the monomethyl and -ethyl esters and monoformate were clarified. In contrast to the fast equilibration of the monoesterification, diesterification did not proceed by the reaction with alcohol. Bulky compounds, such as secondary alcohols, tertiary alcohols, and acetic acid, hardly reacted with the bis-(μ-hydroxo) divanadium site ($K < 0.01$) because of the steric crowding. The *K* values for the other hydroxo compounds decreased in the same order for primary alcohols, including non- and para-substituted benzyl alcohols ≥ water ≫ formic acid, as that for the pK_a values.

Acknowledgment. This work was supported in part by the Core Research for Evolutional Science and Technology (CREST) program of the Japan Science and Technology Agency (JST) and a Grant-in-Aid for Scientific Research from the Ministry of Education, Culture, Science, Sports and Technology of Japan.

Supporting Information Available: X-ray crystallographic files for CEK−**II**, TMA−**III**, TMA−**IV**, and TEA−**V** in CIF format and Figures S1−S9. This material is available free of charge via the Internet at http://pubs.acs.org.

IC051163X

---

(41) Rocchiccioli-Deltcheff, C.; Fournier, M.; Franck, R.; Thouvenot, R. *Inorg. Chem.* **1983**, *22*, 207.

(42) The exchange of oxygen atoms in the V−(μ-OH)$_2$−V site was also supported by the quantum chemical calculation. The IR pattern was calculated with Hartree−Fock level theory. The scaling factor was set to be 0.900, which best reproduced the frequencies of the ν(W−O−W) and ν(Si−O) bands of α-$SiW_{12}O_{40}{}^{4-}$. At this level, the calculated frequencies of ν(W═O), ν(Si−O), ν(W−Oc−W), and ν(W−Oe−W) were 1008, 928, 870, and 801 cm^{-1}, respectively, while the experimental values were 967, 920, 883, and 797 cm^{-1}.[41] While this calculation substantially overestimated the ν(W═O) frequency, the calculated ν(Si−O), ν(W−Oc-W), and ν(W−Oe-W) frequencies fairly reproduced the experimental values within an error of ±13 cm^{-1}. In the case of γ-$SiV_2W_{10}O_{38}(\mu\text{-}OH)_2{}^{4-}$, the calculated IR pattern also fairly agreed the observed spectrum except the ν(M═O) region (>950 cm^{-1}), and the bands experimentally observed at 843 and 699 cm^{-1} were calculated at 828 and 683 cm^{-1}. The respective calculated isotope shifts of these bands for γ-$SiV_2W_{10}O_{38}(\mu\text{-}{}^{18}OH)_2{}^{4-}$ were -1.5 and -3.6 cm^{-1}, and they agreed with experimental -2 and -3 cm^{-1}. The shifts of the other oxygen sites in **I** with ^{18}O exchange were much larger.